

www.acsabm.org Article

Poly(oxanorbornene)-Coated CdTe Quantum Dots as Antibacterial Agents

Denise N. Williams, Julia S. Saar, Vera Bleicher, Sibylle Rau, Karen Lienkamp, and Zeev Rosenzweig*



Cite This: ACS Appl. Bio Mater. 2020, 3, 1097–1104



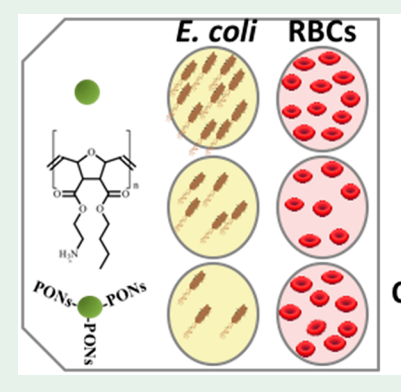
ACCESS

III Metrics & More



Supporting Information

ABSTRACT: In this study, synthetic mimics of antimicrobial peptides based on poly(oxanorbornene) molecules (or PONs) were used to coat CdTe quantum dots (QDs). These PONs-CdTe QDs were investigated for their activity against *Escherichia coli*, a bacterium with antibiotic resistant strains. At the same time, the antibacterial activity of the PONs-CdTe QDs was compared to the antibacterial activity of free PONs and free CdTe QDs. The observed antibacterial activity of the PONs-CdTe QDs was additive and concentration dependent. The conjugates had a significantly lower minimum inhibitory concentration (MIC) than the free PONs and QDs, particularly for PONs-CdTe QDs which contained PONs of high amine density. The maximum activity of PONs-CdTe QDs was not realized by conjugating PONs with the highest intrinsic antibacterial activity (i.e., the lowest MIC in solution as



The therapeutic index of PONs-QDs (bottom) is greater than the therapeutic indices of free QDs (top) and free PONs (middle).

free PONs), indicating that the mechanism of action for free PONs and PONs-CdTe QDs is different. Equally important, conjugating PONs to CdTe QDs decreased their hemolytic activity against red blood cells compared to free PONs, lending to higher therapeutic indices against *E. coli*. This could potentially enable the use of higher, and therefore more effective, PONs-QDs concentrations when addressing bacterial contamination, without concerns of adverse impacts on mammalian cells and organisms.

KEYWORDS: antibacterial agents, bacteria, human red blood cells, quantum dots, antimicrobial polymer, therapeutic index, light activated

■ INTRODUCTION

The increasing prevalence of drug-resistant bacteria has become a global public health challenge. ^{1–5} In the U.S. alone, more than 2.8 million people are infected with drug-resistant bacteria each year; lending to about 35 000 deaths. 4-9 The overwhelming problem of drug-resistant bacterial infections intensifies the need for the development of new antibacterial agents, such as antibacterial polymers and nanoparticles. As with molecular antibiotics, these alternative candidates have the greatest outcomes if they are multitargeting, inhibit bacteria from mounting self-defense mechanisms, and are not readily recognized by efflux pumps. 10 Antibacterial polymer and nanoparticle conjugates with the aforementioned properties have been investigated for potential use in hospital and dentistry settings where antibacterial surface and wound treatments are essential to preventing the spread of drug-resistant bacteria between immune compromised patients. 6,11,12

In general, the conjugation of antibacterial entities to nanoparticles has had mixed results. The conjugates range between being synergistic, effective treatments toward a specific bacterial target, and being completely antagonistic with the properties of the surface bound antibacterial being disrupted by the conjugation. 9,10,13-20 Broad-spectrum synergistic activity

has been realized by conjugating cationic peptides, 13 the photosynthesizer toluidine blue O, 14 functionalized thiol molecules, ¹⁰ small molecule antibiotics (ceftriaxone, ¹⁵ polymyxin-B, ¹⁶ vancomycin, ⁹ indolicidin, ¹⁷ and penicillin ¹⁸), and other antibacterial entities to different nanomaterials. When synergism was observed, nanoparticles enhanced the activity of the conjugated antibacterial due to (a) the combination of the nanoparticles' inherent activity with the activity of their antibacterial coating, (b) the high localized delivery of the conjugated antibacterial molecules to the bacterial targets, and (c) the reorganization of the antibacterial agent into conformations with increased antibacterial activity after conjugation to the nanoparticles' surface. In contrast, there are other examples where conjugating antibacterial agents to nanoparticles has diminished their antibacterial activity. For example, zinc oxide nanoparticles have been shown to decrease the activity of amoxicillin, penicillin, nitrofurantoin, vancomy-

Received: November 14, 2019 Accepted: January 1, 2020 Published: January 1, 2020



cin, and carbenicillin against *Staphylococcus aureus* and the activity of erythromycin against *Escherichia coli.* 19,20 Other potential problems with the conjugation of antibacterial molecules to nanoparticles include a decreased uptake rate and the emergence of off-target toxicity which is introduced by the nanoparticles. 20

This study combines the antibacterial mechanisms of an amine-rich cationic polymer, which is based on its electrostatic and hydrophobic interactions with bacterial cell membranes, with the antibacterial activity of CdTe semiconductor QDs, which is due to reactive oxygen species (ROS) generation. The poly(oxanorbornene)-based synthetic mimics of antimicrobial peptides, or PONs, are facially amphiphilic polymers with tunable hydrophobicity due to varying combinations of a charged ammonium-terminated side chain and a hydrophobic alkyl side chain in each repeat unit.²¹ (See Supporting Information (SI) for synthesis and amine content details). The polymer's mechanism of antibacterial activity involves the positive side chains of the molecule attracting it to the negatively charged bacterial outer envelope, and then the alkyl side chains potentially partitioning into the membrane's hydrophobic interior.²⁴ PONs of appropriate amphiphilicity have shown selective, broad-spectrum activity against bacteria as free molecules and surface-attached polymer networks. 6,11,22-26 Further, a recent study in our lab with PONs-conjugated gold nanoparticles has shown that their conjugation to nanoparticles enhances their membrane penetration activity.²⁷ In the current study, we conjugated the antibacterial PONs to CdTe QDs with a bandgap of 2.4 eV. These QDs were previously shown to have antibacterial activity in the dark which can be enhanced by irradiation with UV light due to increased ROS generation.²⁸ We hypothesized that the cationic side chains of the PONs surface coating will facilitate the attachment of PONs-CdTe QDs to the bacterial cells, the hydrophobic side chains will enable membrane penetration and disruption, and the CdTe QDs will generate ROS in close proximity to cell membranes and organelles to induce bacterial cell death. This paper focuses on the impact of varying the amine content of PONs on the antibacterial and hemolytic activity of PONs-CdTe QDs, with and without light irradiation, and compares the activity of the PONs-CdTe QDs to the antibacterial activity of free PONs and QDs.

MATERIALS AND METHODS

Materials and Reagents. Cadmium chloride (CdCl₂), 3mercaptoundecanoic acid (MPA), sodium citrate dihydrate sodium borohydride (Na₂BH₄), 1-ethyl-3-(3-(dimethylamino)propyl) carbodiimide (EDC), Triton X-100, 2',7'-dichlorofluorescein (H2DCF), sodium phosphate monohydrate, AlamarBlue and melittin were obtained from Sigma-Aldrich. Sodium hydroxide (NaOH) was obtained from Acros Organic. Sodium tellurite was obtained from Alfa Aeser. Tris buffer was obtained from AppliChem. Aqua (sterile water) was obtained from BBraun. Mueller Hinton Broth (MHB) was obtained from BD Difco. EDTA-blood was either drawn fresh every day of assay from an approved volunteer or purchased from Innovative Research, Inc. (Michigan, U.S.). E. coli (Strain ATCC25922) cells were purchased from the Leibniz-Institute DSMZ. Poly(oxanorbornenes) (PONs) were synthesized and characterized as reported previously (see SI for details). 21,23 An Ultrathin LED Light Panel (Neutral White) was purchased from Environmental Lights, San Diego, CA.

Ethics Statement. Red blood cells that were drawn the day of some hemolytic assays were obtained from human volunteers who had previously given their written consent according to the Helsinki declaration, which was approved by the Ethics Board of the Albert-Ludwigs University, Freiburg, Germany.

Synthesis and Characterization of MPA-CdTe Core Quantum Dots. 29 Into a 35 mL microwave vessel with a stir bar, 48.5 mg $CdCl_{2}$ 100 mg sodium citrate dehydrate, 26 μ L of MPA, and 25 mL Millipore water were combined. The pH of this mixture was brought to 10.5 using 1 M NaOH, and then 11 mg of sodium tellurite and 18.9 mg of sodium borohydride were added. The vessel was capped and placed in a CEM Discover SP microwave synthesizer. The mixture was microwaved in Dynamic Mode at 100 °C, 250 psi, 300 W power, and high stirring for 10 min. QDs were purified three times via centrifugation through a 30K MWCO centrifuge filter at 2000g for 5 min, and finally redispersed in pH 10.5 Millipore water. Absorbance properties were detected with a Thermo Scientific Evolution 201 UV-Vis spectrophotometer. The absorbance was used to determine QDs' molar concentration and size according to the literature. 30 Fluorescence spectroscopy measurements were collected using a PTI-Horiba QuantaMaster 400 fluorimeter. High-resolution transmission electron microscopy (HRTEM) images of QDs, that were drop-coated onto mesh copper grids with ultrathin carbon film on holey carbon support film (Ted Pella, Inc.), were obtained using a Titan 80-300 S/TEM, operating at 300 kV with a Gatan OneView imaging camera. Dynamic Light Scattering (DLS) measurements of MPA-QDs were performed using a Malvern Zetasizer Nano ZS instrument.

Coupling PONs to the CdTe Core QDs. PONs were conjugated to the QDs' surface via EDC methods, similar to coupling reported for gold nanoparticles. ²⁷ 10 nmoles of purified CdTe cores were added to a 20 mL vial with a stir bar with 3 mL 0.1 M MES buffer (pH 5), and 5 mg of PONs. While stirring, 50 μ L of 0.2 M EDC was added to the QD solution. The reaction was allowed to go overnight and then ran through a prerinsed 30k MWCO centrifugal filter to rid of excess reactants. Cleaned PONs-QDs conjugates were suspended in fresh 0.1 M MES buffer.

 ζ -Potential Measurements of MPA-QDs and PONs-QDs. ζ -potential measurements were performed using a Malvern Zetasizer Nano ZS instrument. Samples were measured in triplicate using disposable Malvern Zetasizer Nano Series folded capillary cells (DTS1070).

Thermogravimetric Analysis (TGA) of MPA-QDs and PONs-QDs. Prior to TGA, MPA-QDs, and PONs-QDs were pelleted via centrifugation at 2000g for 5 min and the supernatant was removed. The pellets were suspended in minimal Millipore water for transfer to a TGA heating pan, which was placed into a PerkinElmer Pyris 1 thermogravimetric analysis instrument. The pan was heated for 15 min at 100 °C to evaporate the water. Then the temperature was ramped from 100 to 900 °C at 25 °C/min. The mass loss between 100 and 700 °C was used to determine the total amount of MPA and PONs originally on the nanoparticle surface.

H₂DCF Fluorescence Detection of ROS Assay. H₂DCF was used to detect the inherent ROS generation of MPA-QDs and PONs-QDs following the procedures of a previously reported cell-free assay. ³¹ A 50 μ M H₂DCF in Millipore water solution was prepared under inert gas. In 96 well plates, duplicate samples consisted of 100 μL of the 50 μM H_2DCF , 90 μ L Millipore water, and 10 μ L of the respective MPA-QDs and PONs-QDs samples. Concentrations for the PONs-QDs ranged from 6.25 to 400 μ g/mL PONs equivalents, and MPA-QDs equivalents in both the PONs- and MPA- QDs samples ranged from 12.5 to 800 nM in these wells. ROS generated from MPA-QDs and PONs-QDs, with and without irradiation with a neutral white LED plate, was detected in a Molecular Devices SpectraMax M5Microplate reader with λ_{ex} : 495 nm, $\lambda_{\rm em}$: 500–600 nm in relative fluorescence units. An initial reading was read, and followed by a reading every hour for 6 h in the plate reader. These readings were also measured with a PTI-Horiba QuantaMaster 400 fluorimeter under the same conditions for MPA-QDs and H₂DCF control samples.

Minimum Inhibitory Concentration (MIC) Assay with *E. coli*. MIC assays were performed, as previously reported, 32 in a MHB system (pH 7.3). In short, bacteria culture was inoculated overnight in 5 mL of MHB at 37 °C. After shaking overnight at 70 rpm, 500 μ L of the bacteria suspension was transferred to an Eppendorf tube and centrifuged at 8000 rpm for 1.5 min. The supernatant was removed, and the bacterial pellet was resuspended in fresh MHB. These washed

cells were diluted to a final OD_{595} of 0.001 -corresponding to a bacterial concentration of about 10⁶ cells/mL- and then 190 µL was transferred to each appropriate well in 96 well plates. Next, 10 μ L of polymer, QDs, polymer-QDs, and controls of stock concentrations were pipetted into well plates in duplicates (one duplicate = one biological replicate). The final well concentrations of free PONs and PONs-QDs samples ranged from 6.25 to 400 μ g/mL PONs equivalents. The final well concentrations of MPA-QDs and PONs-QDs samples ranged from 0.001 to 1 μ M QD equivalents. Plates were mixed well before placing in a 37 $^{\circ}$ C incubator. After incubating overnight, the OD₅₉₅ was evaluated to quantify bacteria cell viability. For exposures with irradiation, plates were rested directly on top of the neutral white light LED plate for 2 h at the beginning of the incubation in the 37 °C incubator. The 50% amine propyl PONs was used as a positive control in this assay. MES buffer and DMSO were tested with bacteria to ensure the solvents alone did not influence bacteria growth. MHB alone, and with DMSO and MES buffer addition were tested as a negative controls. Further details can be found in the SI.

Hemolysis Assay. Hemolysis assays were performed, as previously reported, 32 in a Tris buffer system (pH 7.0). In short, 30 μ L of EDTAblood with 10 mL of Tris buffer, per 96 well plate, was centrifuged at 3000 rpm for 5 min. The supernatant was removed from the red blood cell (RBC) pellet. Ten mL of Tris buffer was added to resuspend the pellet, and this washing was repeated for three total wash and resuspension cycles. The number of RBCs was counted using a Neubauer chamber to check for blood quality. 160 μ L of the RBCs in Tris buffer solution was added to each sample well in duplicates (one duplicate = one biological replicate). 40 μ L of the sample or control was added to each well; for a total well volume of 200 μ L. The final well concentrations of free PONs and PONs-QDs samples ranged from 0.1 to 8000 µg/mL PONs equivalents. The final well concentrations of MPA-QDs and PONs-QDs samples ranged from 0.001 to 10 μ M QD equivalents. Plates were incubated at 30 °C for 30 min, and then centrifuged at 3000 rpm for 5 min. 100 µL of the supernatant was transferred via multichannel pipet to new plates and then analyzed for OD₄₁₄. A 10% Triton-X solution was used as positive control in this assay. Agua, MES buffer and DMSO were used as negative controls. Tris buffer was tested as a solution blank. Further details can be found in the SI.

RESULTS AND DISCUSSION

Synthesis and Physical Characterization. Free Poly-(oxanorbornene)(PONs) and Mercaptopropionic Acidcoated CdTe Quantum Dots (MPA-CdTe QDs). For this study, a series of four PONs molecules with 10 repeat units each, but varying amine content (55-100%), were synthesized from two different comonomers by adjusting the comonomer ratios during polymerization (SI Figures S1-S3). The different PONs obtained were each conjugated to microwave synthesized MPA-CdTe QDs. Prior to conjugation, the MPA-CdTe QDs were characterized using UV-vis spectroscopy, fluorescence spectroscopy, DLS, and HRTEM measurements. Figure 1 and SI Figure S4 show the results these optical characterizations. Figure 1A shows the normalized absorbance and emission spectra of the microwave synthesized CdTe QDs. The QDs have a first excitonic peak at 510 nm and an emission maximum at 578 nm. Using published calculations for absorbance data, the 510 nm first exciton was found to correspond to 2.6 nm diameter CdTe crystals, with 2.4 eV bandgaps. 30 Figure 1B shows the DLSdetermined number size distribution of the MPA-QDs in pH 11 Millipore water. The hydrodynamic diameter of these MPA-QDs was determined to be 5.0 ± 1.5 nm. The supplementary graphs of SI Figure S4 show complementary size characterizations of these MPA-QDs obtained through DLS measurements at pH 7 and HRTEM imaging. As reactive oxygen species (ROS) generation is the predominant antibacterial mechanism of action for semiconductor nanomaterials like CdTe QDs, 28 it

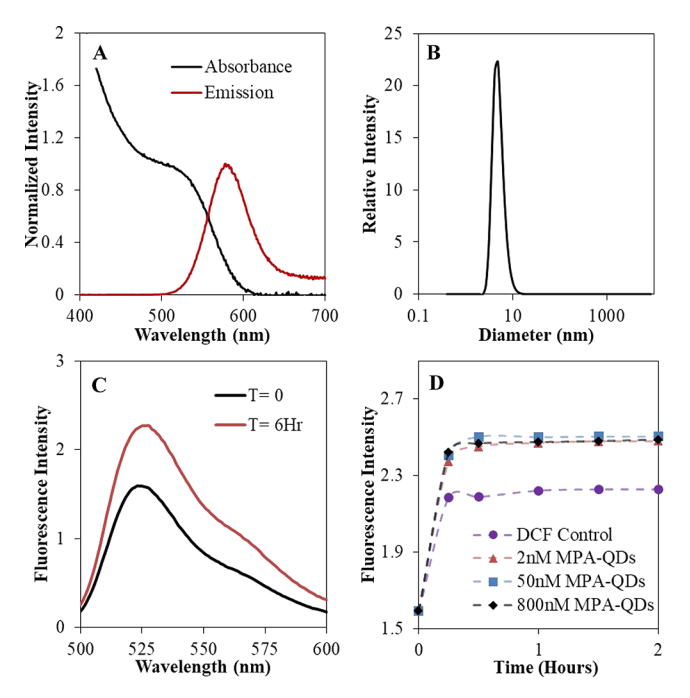


Figure 1. Optical properties of MPA-CdTe QDs. (A)Normalized absorbance and emission ($\lambda_{\rm ex}=375~{\rm nm}$) spectra of the microwave synthesized CdTe QDs used in this study show that the QDs have a first excitonic peak at 510 nm and an emission maximum at 578 nm. (B)DLS-measured number size distribution of MPA-QDs determined their hydrodynamic diameter to be 5.0 \pm 1.5 nm; N=3. (C)Fluorescence emission profile of H₂DCF (t=0, black) compared to the air-oxidation derived DCF (t=6 h, red) ($\lambda_{\rm ex}=495~{\rm nm}$). (D) The rate of the oxidative ROS generation by varying concentrations of MPA-QDs is faster than air oxidation of H₂DCF samples ($\lambda_{\rm ex}=495~{\rm nm}$, $\lambda_{\rm em}=525~{\rm nm}$, N=3).

was investigated using fluorescence spectroscopy (Figure 1C and D). For this, oxidation-dependent changes of the fluorescence spectra of the minimally fluorescent 2',7'dichlorodihydrofluorescein (H2DCF) molecule into the highly fluorescent 2',7'-dichlorofluorescein (DCF) molecule were evaluated. Figure 1C shows a fluorescence emission spectrum of H_2DCF at $t \approx 0$ ($\lambda_{ex} = 495$ nm, black) compared to a spectrum at t = 6 h (λ_{ex} = 495 nm, red) after the dye has been oxidized to DCF by air exposure. The emission increase of this control sample at the emission peak wavelength of 525 nm indicates a slow oxidation of H2DCF to DCF under these experimental conditions. Figure 1D shows the rate of H₂DCF oxidation by air alone as a control (purple) and with increasing concentrations of the free MPA-QDs. MPA-QDs increase the rate of H₂DCF oxidation, with the greatest change happening between 0 and 15 min. There are also minimal increases in the rate of QD ROSinduced oxidation with increasing QD concentration within this time frame. After 30 min, the oxidation of the available H₂DCF by the MPA-QDs is complete, as indicated by the fluorescence of DCF reaching its maximum intensity.

Synthesis of PONs-QDs. Scheme 1 illustrates the covalent conjugation of the above-described PONs to MPA-QDs through 1-ethyl-3-(3-(dimethylamino)propyl)carbodiimide (EDC) coupling of the acid groups on the MPA-QDs to the amine groups of the PONs. PONs molecules of the same chain length have been successfully coupled to ~30 nm diameter gold nanoparticles (AuNPs) via similar methods.²⁷ In this study, conjugation was achieved at a 1:2000:1000 molar ratio of purified MPA-CdTe cores to PONs to EDC molecules. The

Scheme 1. Synthesis of Poly(oxanorbornene)-Coated CdTe Quantum Dots (PONs-QDs).

reagents were stirred overnight in 0.1 M MES buffer. Before characterization and use, the conjugates were purified using a prerinsed 30k MWCO centrifugal filter to remove excess reactants, and then suspended in fresh 0.1 M MES buffer.

Characterization of PONs-QDs. ζ-potential measurements, thermogravimetric analysis (TGA), and fluorescence spectroscopy were used to characterize the QDs before and after PONs conjugation (Figure 2). Figure 2A shows that prior to conjugation, the MPA-QDs were negatively charged with a ζpotential of -38 mV. Following conjugation, the ζ -potential values of PONs-QDs ranged between +15 and +30 mV, which confirms the conjugation of the positively charged PONs to the negatively charged MPA-QDs. Figure 2B shows TGA traces of MPA-QDs (purple) and PONs-QDs with PONs of varying amine/alkyl ratio (red, black, green, and blue; in order of increasing amine content). MPA-QDs showed a mass loss of 29 \pm 2% between 100 and 700 °C due to the desorption of MPA molecules from the QDs' surfaces. When correcting for the 29 \pm 2% mass loss due to the loss of MPA from the QDs, the mass losses due to the desorption of PONs from the PONs-QDs were $54 \pm 8\%$ for the 55% amine PONs (red), $50 \pm 8\%$ for the 75% amine PONs (black), $51 \pm 5\%$ for the 95% amine PONs (green), and $51 \pm 2\%$ for the 100% amine PONs (blue). These values indicate that the surface coverage of PONs on the QDs does not vary significantly even though the PONs have varying amine/alkyl side chain ratios. This contrasts with the previously observed significant dependence of the PONs' surface coverage on their amine/alkyl ratio when conjugated to 30 nm diameter gold nanoparticles.²⁷ These findings suggest that the ratio between the polymer length and the diameter of the nanoparticles also affects the polymer surface coverage of nanoparticles. Since the PONs surface coverage on our CdTe QDs does not significantly depend on the PONs molecular structure, any changes in the activity of PONs-QDs coinciding with varying amine content is due to changes in PONs structure, and not due to differences in surface coverage. Interestingly, with the

similar number of varying amine content PONs per QD we would expect to observe a greater difference in the ζ -potential values between PONs-QDs of varying amine content, but we do not. The fact that we observe very similar charges between the varying amine content PONs-QDs indicates there is a likely a difference in orientation of the PONs on the QDs, as was observed in the PONs-AuNPs study.²⁷ The hydrophilic amine side chains are oriented toward the surrounding solution, whereas the hydrophobic butyl side chains are packed against the QD surface. This would primarily leave only the amine side chains available for detection via ζ -potential measurements, and could explain why there is minimal difference between the varying PONs-QDs ζ-potential values. Figure 2C shows the effect of PONs conjugation on ROS generation from PONs-QDs in the absence (black) and presence (red) of broad white light irradiation from a neutral white LED light panel during incubation. The panel's emission spectrum is shown in SI Figure S5. In agreement with previous studies, ⁷ irradiation of free MPA-QDs increases the ROS generation level by about 25% under our experimental conditions. However, coating CdTe QDs with PONs polymeric ligands prevented the same magnitude of ROS generation that was observed with free MPA-QDs. These observations might be attributed to the restricted access of water molecules, which are required for ROS generation, to the surface of QDs once they are coated with PONs. Further, without irradiation the ROS generation from the PONs-QDs depends on the molecular structure of the PONs. This may be attributed to the access of water molecules to the PONs-QDs' surface being lower with increasing hydrophobicity (decreasing amine content) of the coating PONs. As previously discussed, the lower amine content PONs likely have a tighter packing around the QD surface than the higher amine content PONs, since the lower amine content PONs would have more hydrophobic side chains packed against the QD surface, whereas the higher amine content PONs have more hydrophilic side chains free in the solution. With irradiation, the ROS generation of the higher ACS Applied Bio Materials www.acsabm.org Article

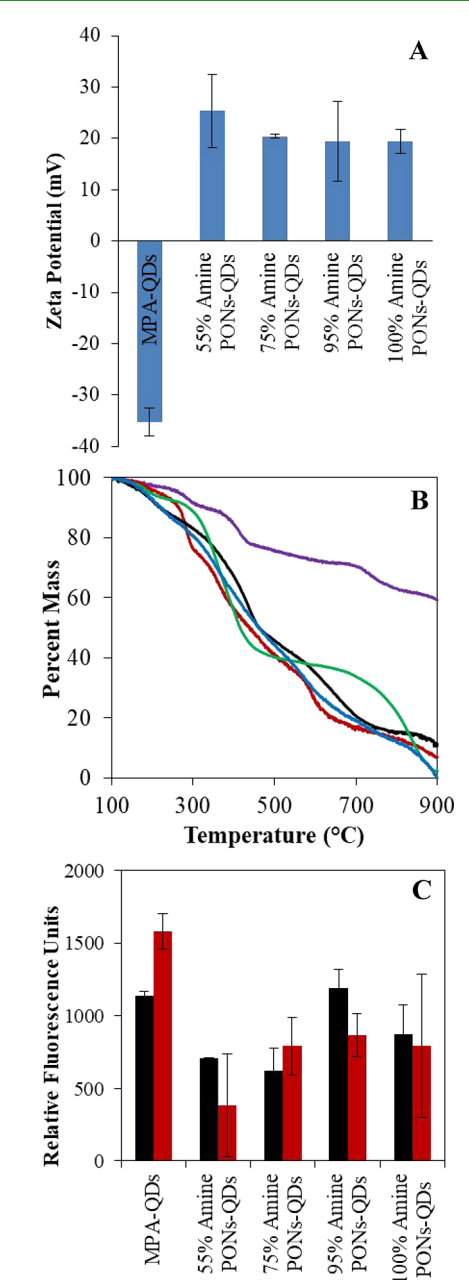


Figure 2. Characterization of MPA-QDs and PONs-QDs with varying amine/alkyl ratio in the conjugated PONs. (A) Zeta potential measurements show MPA-QDs to be negatively charged and PONs-QDs to be positively charged. This confirms the EDC coupling of PONs to MPA-QDs. (B)TGA analysis show similar mass losses due to desorption of 55% (red), 75% (black), 95% (green), and 100% (blue) amine PONs from the surface of MPA-CdTe QDs (purple) with weak dependence (within the error of TGA measurements) on the amine/ alkyl ratio in the conjugated PONs. All mass values were normalized to the mass at 700 °C, a temperature where all organic content is desorbed from the QD surface, for analysis. (C)Cell-free H₂DCF ROS measurements with 6.25 μ g/mL PONs/12.5 nM QDs equivalents and 2 h of incubation demonstrate higher ROS generation levels for free MPA-QDs upon irradiation, but not for PONs-QDs. Further, the ROS levels of PONs-QDs depend on the PONs molecular structure. (N = 3for panels A and B; N = 2 for panel C.).

amine content (75–100%) PONs-QDs increases to similar levels observed for nonirradiated MPA-QDs.

Biological Characterization. Antibacterial Activity of Free PONs. The antibacterial activity (minimum inhibitory concentration, MIC) of the PONs used in this study can be found in the literature. However, for consistent results with our additional data, we repeated these experiments under our experimental conditions, with and without broad white light irradiation from the aforementioned LED panel during incubation. Briefly, SI Figure S6 is 96 well plate schematic for one biological replicate of the MIC assay that was conducted, with samples of varying treatment concentrations and respective controls in duplicates. The antibacterial activity of all treatments (free PONs, free QDs, and PONs-QDs) was quantified in this well plate MIC assay by reading the optical density at 595 nm (OD₅₉₅) of the cellular suspensions after overnight incubation with the varying treatments. Figure 3A shows the normalized bacterial growth (in %) of E. coli when incubated with free PONs of varying amine content and increasing PONs' concentration $(6.25-100 \,\mu\text{g/mL})$ without LED panel irradiation. We did not observe significant changes in the free PONs activity with

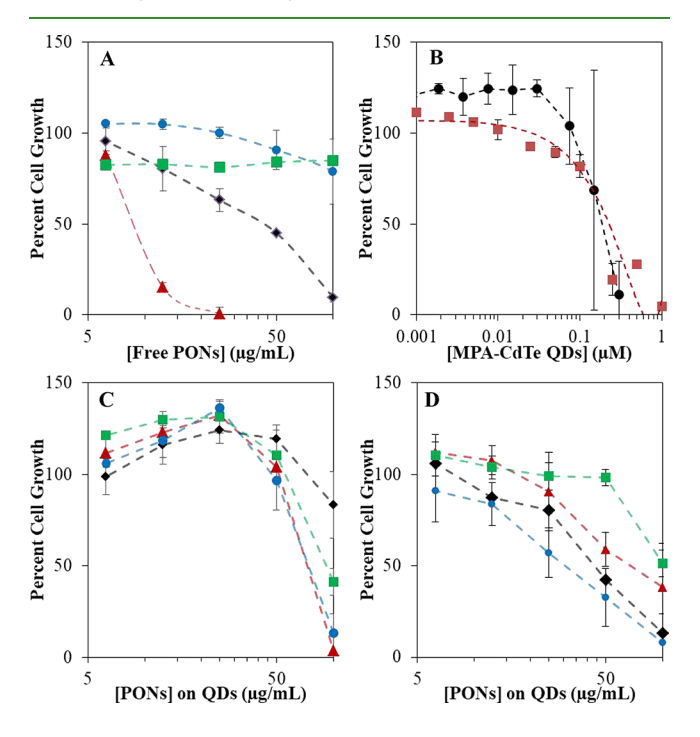


Figure 3. Anti-E. coli activity of PONs, MPA-QDs, and PONs-QDs. Relative E. coli viability (normalized to E. coli grown with solvent controls) represented as percent cell growth versus the concentration of free PONs, free MPA-QDs, or PONs equivalents on the PONs-QDs. (A) Growth of E. coli after incubation with 6.25–100 μ g/mL of free 55% (red triangle), 75% (black diamond), 95% (green square), and 100% (blue circle) amine content PONs show that lower amine content PONs are more active than the higher amine content PONs. (B) E. coli cells show a concentration dependent decrease in growth when exposed to increasing concentrations of free MPA-QDs without irradiation (black circle). Two-hour irradiation (red square) at the beginning of incubation increases the activity of MPA-QDs against *E. coli.* (C and D) Growth of E. coli when incubated with 6.25-100 µg/mL PONs equivalents (corresponding to 12.5-160 nM QD equivalents, as determined by TGA) of 55% (red triangle), 75% (black diamond), 95% (green square), and 100% (blue circle) amine PONs-QDs without (C) and with 2 h irradiation (D) show that higher amine PONs-QDs have increased antibacterial activity compared to their respective free PONs. Lower amine content PONs have decreased activity once conjugated to QDs. $(N \ge 3 \text{ biological replicates.})$.

irradiation (data not shown). Figure 3A curves can be summarized by extrapolating the free PONs' concentration that inhibited at least 90% of bacterial cell growth (MIC $_{90}$). The MIC $_{90}$ values of the free PONs were 12.5 μ g/mL for 55% amine PONs, 100 μ g/mL for 75% amine PONs, and higher than 400 μ g/mL for the 95% and 100% amine PONs. This data shows that the free PONs maintain the literature established trend of the lower amine content PONs having greater activity against bacterial cell growth than the higher amine content PONs. This trend has been attributed to the dependence of PONs' activity on the balance between the prevalence of cationic moieties which are necessary for electrostatic attraction of the PONs molecules to the anionic bacterial membrane, and the hydrophobic moieties which are needed to penetrate the membrane and lead to cell breakdown and death. ²²

Antibacterial Activity of MPA-CdTe QDs. Figure 3B describes the anti-E. coli activity of the MPA-QDs. Per our calculations of PONs coverage, the maximum QD concentration used in the PONs conjugate exposures to bacterial cells was 0.16 μ M, which is below the concentration where there was any significant QD activity against bacterial cells without LED irradiation. Irradiating these QDs with an LED panel in order to light-enhance their generation of ROS showed a modest concentration dependent increase in activity against E. coli growth. This may be explained by the increase in ROS generation with increased QD concentration (Figure 1D). This light-activated antigrowth activity of the QDs is what we aim to combine with the membrane-penetration activity of the PONs molecules in the PONs-QDs conjugates.

Antibacterial Activity of PONs-QDs. The anti-E. coli activity of PONs-QDs with varying PONs molecular structure (amine/ alkyl ratio) were characterized parallel to the MIC assays for free PONs and MPA-QDs described above. Figure 3C and D show dose-response curves of E. coli growth when exposed to 6.25-100 μ g/mL PONs equivalents on the PONs-QDs. Without irradiation (Figure 3C), the PONs equivalent MIC90 values for the conjugates against *E. coli* were 100, 200, 200, and $100 \mu g/mL$ in order of increasing amine content PONs. With irradiation (Figure 3D), the PONs equivalent MIC₉₀ values of 100, 100, 200, and 50 μ g/mL for PONs-QDs, in order of increasing amine/alkyl ratio, demonstrate an irradiation-induced increase in activity against bacterial growth only for PONs-QDs with 75% and 100% amine/alkyl ratios. Regardless of irradiation, the lesser activity of the 55% and 75% amine content PONs as QD conjugates compared to their activity as free PONs coincides with their decreased ROS generation efficiency compared to the free MPA-QDs (Figure 2C). On the contrary, the higher amine content PONs-QDs do not have a significant difference in their ROS generation compared to the MPA-QDs; so their increase in anti-E. coli growth activity, compared to the respective free PONs, can be attributed to the preservation of the ROS generation-based activity of the QDs being combined with the antimembrane activity of the PONs surface coating. Regardless of the use of irradiation, conjugating the higher amine content PONs to QDs increases their activity against E. coli cell growth compared to the same mass used as free PONs.

Hemolytic Activity of Free PONs, MPA-QDs, and PONs-CdTe QDs. The hemolytic activity for all samples was tested in parallel using the hemolytic assay illustrated by SI Figure S7. This figure shows a 96 well plate schematic for one biological replicate of the hemolysis assay, with samples of varying concentration and the hemolytic controls in duplicate. Hemolysis was quantified in this assay by reading the OD₄₁₄

of the red blood cell supernatant. Unconjugated MPA-QDs had negligible hemolytic activity up to 10 μ M (SI Figure S8C). Figure 4 compares the concentration of free PONs and PONs

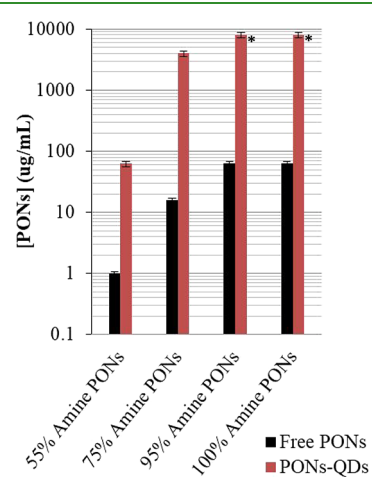


Figure 4. HC $_{50}$ values of PONs-QDs compared to free PONs molecules. After red blood cell exposures to 0.1–8000 μ g/mL PONs equivalents of free PONs and PONs-QDs, the PONs-QDs (red) were found to have lower hemolytic activity than free PONs molecules (black). (N=3 biological replicates.). Note*: HC $_{50}$ values for 95% and 100% Amine PONs-CdTe QDs were not found within the tested concentration range, and are thus represented as bars to the highest tested concentration.

equivalents of PONs-QDs that led to 50% hemolysis (HC_{50}). The corresponding hemolytic curves with PONs concentrations between 0.1 to 8000 μ g/mL, from which the HC₅₀ values were extrapolated, can be found in SI Figure S8. PONs-QDs (Figure 4, red) with PONs of high amine/alkyl ratio show negligible hemolytic activity at all tested concentrations, while 55% amine PONs-QDs had an HC₅₀ of 31.25 μ g/mL PONs equivalents and 75% amine PONs-QDs had an HC₅₀ of 3000 μ g/mL PONs equivalents. The hemolytic activity of the MPA-QDs and PONs-QDs samples were not statistically affected by LED irradiation during incubation with red blood cells (data not shown). The hemolytic activity of all PONs-QDs is at least 2 orders of magnitude lower than that of the free PONs (Figure 4, black) which had measured HC₅₀'s of 1, 15.6, 31.25, and 41 μ g/mL in order of increasing amine content. This major reduction in hemolytic activity upon conjugation is likely observed as the nanoparticle-bound PONs are less able to insert their hydrophobic moieties into the zwitterionic, mammalian membranes. This will be discussed in more detail in the Summary and Conclusions section.

Therapeutic Indices of free PONs vs PONs-CdTe QDs. Taking into consideration the change in antibacterial and hemolytic activities once PONs were conjugated to the MPAQDs, we calculated the therapeutic indices of the PONs-QDs and compared them to the therapeutic indices of free PONs. We defined the therapeutic index as a sample's HC_{50} divided by its MIC_{90} . We calculated the indices for free PONs against *E. coli* to be 0.08 for 55% amine PONs, 0.12 for 75% amine PONs, and inconclusive for 95% and 100% amine PONs due to the lack of antibacterial activity for these two free PONs at tested concentrations. The free PONs tested in this study had a smaller therapeutic window than found in the literature, but the trend of higher amine content PONs having a larger therapeutic index than the smaller amine content PONs remained due to the

higher amine content PONs having a lower hemolytic activity the smaller amine content PONs. With irradiation, the therapeutic indices for PONs-QDs were 0.63, 40, > 40, and >160, in order of increasing amine content. The indices for the PONs-QDs are significantly larger in magnitude than the free PONs therapeutic indices calculated in this study and the literature, especially for the 95% and 100% amine PONs-QDs for which minimal hemolytic activity was detected even though there was antibacterial activity. The lower hemolytic activity of the PONs-QDs compared to free PONs against *E. coli* and the resulting therapeutic index improvement demonstrates the potential for a higher PONs concentration to be used when in conjugate form (rather than free polymer form).

SUMMARY AND CONCLUSIONS

A series of PONs with varying amine/alkyl ratios was conjugated to the surface of CdTe QDs in order to study the PONs-QDs conjugates' antibacterial and hemolytic activity. Prior to conjugation, the free PONs' antibacterial and hemolytic activity decreased with the amine content increasing from 55% to 100%, in agreement with previous studies.⁶ Prior to conjugation, the free MPA-QDs at a concentration range of 1-160 nM only exhibited significant antibacterial activity when they were irradiated. MPA-QDs at this concentration range had no significant hemolytic activity with or without irradiation. While PONs conjugation to the surface of the CdTe QDs resulted in a general loss of the trend of amine-content dependent antibacterial activity, we did observe comparable antibacterial activity of the conjugates to that of the free PONs of similar PONs mass which could be enhanced with irradiation. Alongside this result of conjugation was the outcome that the levels of hemolytic activity of the PONs-QDs toward mammalian cells were dramatically reduced, especially for the higher amine content PONs-containing conjugates. The decrease in hemolytic activity is most likely due to the restricted motility of the PONs and the QD surface-hugging orientation of the hydrophobic butyl side chains once the PONs are surfaceattached, resulting in a lower effective concentration of hydrophobic groups interacting with the mammalian cell membrane. Numerous studies have shown that synthetic mimics of antimicrobial peptides become toxic (at the same cationic charge density) when they are too hydrophobic, for example, when the length of the alkyl side chain is increased by one repeat unit.⁶ This is because an increased hydrophobicity results in an increased partitioning of these surface-active molecules into the hydrophobic part of the mammalian cell membrane. Thus, a decrease in toxicity of the nanoparticle-bound PONs can be interpreted as a reduced effective hydrophobicity compared to free PONs. On the other hand, the antibacterial activity of the amine-rich and more hydrophilic PONs on the QDs is enhanced when surface-attached. This could be because there are more hydrophilic amine/ammonium groups directed toward the aqueous medium (not buried inside the interface like the hydrophobic groups), and because the interaction between PONs-QDs with the negatively charged bacterial membranes is charge driven. While a free PONs molecule has only a few charges under physiological conditions, the surface-bound PONs behave like polyelectrolytes, which strongly enhances their interaction with the bacterial cells. The reduced hemolytic activity has led to an increase in the therapeutic indices of PONs-QDs conjugates against E. coli, especially for higher amine content PONs-QDs. The larger therapeutic indices may enable the use of PONs-QDs at greater and more effective

concentrations against antibiotic-resistant gram-negative bacteria, such as *E. coli*, with reduced concerns about hemolytic and toxic activity against mammalian cells. Additional studies should be conducted, first with other *E. coli* strains and then with other gram-negative bacterial strains, to find out how general the impact of PONs conjugation to QDs is on their antibacterial activity.

ASSOCIATED CONTENT

Solution Supporting Information

The Supporting Information is available free of charge at https://pubs.acs.org/doi/10.1021/acsabm.9b01045.

Butyl poly(oxanorbornene) polymers (PONs) synthesis and characterization (Figures S1–S3, Tables S1–S2), additional characterization of the MPA-QDs (Figure S4), LED panel characterization (Figure S5), minimum inhibitory concentration (MIC) assay with *E. coli* (Figure S6, Table S3), human red blood cell lysis (hemolysis) assay (Figure S7), hemolytic activity of free PONs, MPA-QDs, and PONs-QDs (Figure S8), therapeutic indices of free PONs, PONs-QDs and MPA-QDs (Table S4) (PDF)

AUTHOR INFORMATION

Corresponding Author

Zeev Rosenzweig — University of Maryland, Baltimore County, Baltimore, Maryland; o orcid.org/0000-0001-6098-3932; Email: zrosenzw@umbc.edu

Other Authors

Denise N. Williams — University of Maryland, Baltimore County, Baltimore, Maryland; orcid.org/0000-0002-6314-2052

Julia S. Saar – Albert-Ludwigs-Universität, Freiburg, Germany

Vera Bleicher – Albert-Ludwigs-Universität, Freiburg, Germany

Sibylle Rau – Faculty of Medicine, Albert-Ludwigs-Universität, Freiburg, Germany

Karen Lienkamp — Albert-Ludwigs-Universität, Freiburg, Germany; ⊚ orcid.org/0000-0001-6868-3707

Complete contact information is available at: https://pubs.acs.org/10.1021/acsabm.9b01045

Notes

The authors declare no competing financial interest.

ACKNOWLEDGMENTS

This work was primarily supported by National Science Foundation grant number CHE-1904600 and an AGEP graduate fellowship supplement award for D.N.W. Work in collaboration with the Lienkamp group was additionally supported by the National Science Foundation Center for Chemical Innovation (CCI) program award for the Center for Sustainable Nanotechnology (CSN) under grant number CHE-1503408. We also acknowledge Dr. Viknesh Sivanathan and the HHMI Science Education group at UMBC for availability of their microbiology facilities, the UMBC Molecular Characterization nad Ananlysis Complex for training on and availability of TGA instrumentation, and Dr. Alline Myers of the National Institute of Standard and Technology (NIST) Center for

nanoscale Science and Technology for assistance with TEM imaging.

REFERENCES

- (1) World Health Organization, AntimicrobialResistance: Global Report on Surveillance; WHO Press, 2014.
- (2) National Institute of Allergy and Infectious Diseases NIAID Antimicrobial Resistance Program: Current Status and Future Directions, 2014
- (3) Laxminarayan, R.; Amábile-Cuevas, C. F.; Cars, O.; Evans, T.; Heymann, D. L.; Hoffman, S.; Holmes, A.; Mendelson, M.; Sridhar, D.; Woolhouse, M.; Røttingen, J.-A. UN High-Level Meeting on antimicrobials—what do we need? *Lancet* **2016**, 388 (10041), 218–220
- (4) Center for Disease Control and Prevention Antibiotic resistance threats in the United States, 2019; CDC: Atlanta; 2019.
- (5) Lushniak, B. D. Antibiotic resistance: a public health crisis. *Public Health Rep.* **2014**, 129 (4), 314–316.
- (6) Al-Ahmad, A.; Laird, D.; Zou, P.; Tomakidi, P.; Steinberg, T.; Lienkamp, K. Nature-Inspired Antimicrobial Polymers Assessment of Their Potential for Biomedical Applications. *PLoS One* **2013**, *8* (9), No. e73812.
- (7) Courtney, C.; Goodman, S.; McDaniel, J.; Madinger, N.; Chatterjee, A.; Nagpal, P. Photoexcited quantum dots for killing multidrug-resistant bacteria. *Nat. Mater.* **2016**, *15* (5), 529–534.
- (8) Thayer, A. Will the bugs always win? *Chem. Eng. News* **2016**, 94 (35), 36–43.
- (9) Chen, H.; Zhang, M.; Li, B.; Chen, D.; Dong, X.; Wang, Y.; Gu, Y. Versatile antimicrobial peptide-based ZnO quantum dots for in vivo bacteria diagnosis and treatment with high specificity. *Biomaterials* **2015**, 53, 532–544.
- (10) Bresee, J.; Bond, C.; Worthington, R.; Smith, C.; Gifford, J.; Simpson, C.; Carter, C.; Wang, G.; Hartman, J.; Osbaugh, N.; Shoemaker, R.; Melander, C.; Feldheim, D. Nanoscale Structure-Activity Relationships, Mode of Action, and Biocompatibility of Gold Nanoparticle Antibiotics. *J. Am. Chem. Soc.* **2014**, *136* (14), 5295–5300
- (11) Kurowska, M.; Eickenscheidt, A.; Guevara-Solarte, D.; Widyaya, V.; Marx, F.; Al-Ahmad, A.; Lienkamp, K. A Simultaneously Antimicrobial, Protein-Repellent, and Cell-Compatible Polyzwitterion Network. *Biomacromolecules* **2017**, *18* (4), 1373–1386.
- (12) Hartleb, W.; Saar, J.; Zou, P.; Lienkamp, K. Just Antimicrobial is not Enough: Toward Bifunctional Polymer Surfaces with Dual Antimicrobial and Protein-Repellent Functionality. *Macromol. Chem. Phys.* **2016**, 217 (2), 225–231.
- (13) Liu, L.; Xu, K.; Wang, H.; Tan, P.; Fan, W.; Venkatraman, S.; Li, L.; Yang, Y. Self-assembled cationic peptide nanoparticles as an efficient antimicrobial agent. *Nat. Nanotechnol.* **2009**, *4* (7), 457–463.
- (14) Narband, N.; Mubarak, M.; Ready, D.; Parkin, I.; Nair, S.; Green, M.; Beeby, A.; Wilson, M. Quantum dots as enhancers of the efficacy of bacterial lethal photosensitization. *Nanotechnology* **2008**, *19* (44), 445102.
- (15) Luo, Z.; Wu, Q.; Zhang, M.; Li, P.; Ding, Y. Cooperative antimicrobial activity of CdTe quantum dots with rocephin and fluorescence monitoring for Escherichia coli. *J. Colloid Interface Sci.* **2011**, 362 (1), 100–106.
- (16) Park, S.; Chibli, H.; Wong, J.; Nadeau, J. Antimicrobial activity and cellular toxicity of nanoparticle-polymyxin B conjugates. *Nanotechnology* **2011**, 22 (18), 185101.
- (17) Galdiero, E.; Siciliano, A.; Maselli, V.; Gesuele, R.; Guida, M.; Fulgione, D.; Galdiero, S.; Lombardi, L.; Falanga, A. An integrated study on antimicrobial activity and ecotoxicity of quantum dots and quantum dots coated with the antimicrobial peptide indolicidin. *Int. J. Nanomed.* **2016**, *11*, 4199–4211.
- (18) Turos, E.; Reddy, G.; Greenhalgh, K.; Ramaraju, P.; Abeylath, S.; Jang, S.; Dickey, S.; Lim, D. Penicillin-bound polyacrylate nanoparticles: Restoring the activity of beta-lactam antibiotics against MRSA. *Bioorg. Med. Chem. Lett.* **2007**, *17* (12), 3468–3472.

- (19) Banoee, M.; Seif, S.; Nazari, Z. E.; Jafari-Fesharaki, P.; Shahverdi, H. R.; Moballegh, A.; Moghaddam, K. M.; Shahverdi, A. R. ZnO nanoparticles enhanced antibacterial activity of ciprofloxacin against Staphylococcus aureus and Escherichia coli. *J. Biomed. Mater. Res., Part B* **2010**, 93 (2), 557–61.
- (20) Allahverdiyev, A. M.; Kon, K. V.; Abamor, E. S.; Bagirova, M.; Rafailovich, M. Coping with antibiotic resistance: combining nanoparticles with antibiotics and other antimicrobial agents. *Expert Rev. Anti-Infect. Ther.* **2011**, *9* (11), 1035–1052.
- (21) Lienkamp, K.; Madkour, A.; Musante, A.; Nelson, C.; Nusslein, K.; Tew, G. Antimicrobial polymers prepared by ROMP with unprecedented selectivity: A molecular construction kit approach. *J. Am. Chem. Soc.* **2008**, *130* (30), 9836–9843.
- (22) Lienkamp, K.; Kumar, K.; Som, A.; Nusslein, K.; Tew, G. Doubly Selective" Antimicrobial Polymers: How Do They Differentiate between Bacteria? *Chem. Eur. J.* **2009**, *15* (43), 11710–11714.
- (23) Lienkamp, K.; Madkour, A.; Kumar, K.; Nusslein, K.; Tew, G. Antimicrobial Polymers Prepared by Ring-Opening Metathesis Polymerization: Manipulating Antimicrobial Properties by Organic Counterion and Charge Density Variation. *Chem. Eur. J.* **2009**, *15* (43), 11715–11722.
- (24) Lienkamp, K.; Tew, G. Synthetic Mimics of Antimicrobial Peptides-A Versatile Ring-Opening Metathesis Polymerization Based Platform for the Synthesis of Selective Antibacterial and Cell-Penetrating Polymers. *Chem. Eur. J.* **2009**, *15* (44), 11784–11800.
- (25) Zou, P.; Hartleb, W.; Lienkamp, K. It takes walls and knights to defend a castle synthesis of surface coatings from antimicrobial and antibiofouling polymers. *J. Mater. Chem.* **2012**, 22 (37), 19579–19589.
- (26) Zou, P.; Laird, D.; Riga, E.; Deng, Z.; Dorner, F.; Perez-Hernandez, H.; Guevara-Solarte, D.; Steinberg, T.; Al-Ahmad, A.; Lienkamp, K. Antimicrobial and cell-compatible surface-attached polymer networks how the correlation of chemical structure to physical and biological data leads to a modified mechanism of action. *J. Mater. Chem. B* **2015**, *3* (30), 6224–6238.
- (27) Zheng, Z.; Saar, J.; Zhi, B.; Qiu, T. A.; Gallagher, M. J.; Fairbrother, D. H.; Haynes, C. L.; Lienkamp, K.; Rosenzweig, Z. Structure—Property Relationships of Amine-rich and Membrane-Disruptive Poly(oxonorbornene)-Coated Gold Nanoparticles. *Langmuir* **2018**, 34 (15), 4614—4625.
- (28) Lu, Z.; Li, C.; Bao, H.; Qiao, Y.; Toh, Y.; Yang, X. Mechanism of antimicrobial activity of CdTe quantum dots. *Langmuir* **2008**, 24 (10), 5445–5452.
- (29) Wang, K.; Li, N.; Hai, X.; Dang, F. Lysozyme-mediated fabrication of well-defined core—shell nanoparticle@metal—organic framework nanocomposites. *J. Mater. Chem. A* **2017**, *S* (39), 20765—20770
- (30) Yu, W.; Qu, L.; Guo, W.; Peng, X. Experimental determination of the extinction coefficient of CdTe, CdSe and CdS nanocrystals (vol 15, pg 2854, 2003). *Chem. Mater.* **2004**, *16* (3), 560–561.
- (31) Roesslein, M.; Hirsch, C.; Kaiser, J.-P.; Krug, H. F.; Wick, P. Comparability of in vitro tests for bioactive nanoparticles: a common assay to detect reactive oxygen species as an example. *Int. J. Mol. Sci.* **2013**, *14* (12), 24320–24337.
- (32) Al-Ahmad, A.; Laird, D.; Zou, P.; Tomakidi, P.; Steinberg, T.; Lienkamp, K. Nature-Inspired Antimicrobial Polymers Assessment of Their Potential for Biomedical Applications. *PLoS One* **2013**, *8* (9), No. e73812.